International Journal of Control, Automation, and Systems (2013) 11(1):216-224 ISSN:1598-6446 eISSN:2005-4092
DOI 10.1007/s12555-011-9202-x http://www.springer.com/12555

Visual Cooperation Based on LOS for Self-organization of Swarm Robots

Hahmin Jung, Yeongyun Kim, and Dong Hun Kim*

Abstract: In this study, an attempt has been made to incorporate visual cooperation among decentralized swarm robots for self-organization. Self-organization based on color recognition is presented to overcome the constraints faced in conventional self-organization based on centralized control, in which an external ceiling camera or beacon systems are used. In the proposed scheme, a singular association rule is introduced: a swarm robot considers line-of-sight (LOS) visual information only about its reference robot or a moving target. In particular, this paper presents the following set of cases pertaining to self-organization of swarm robots: 1) a case in which a robot loses a moving target from its LOS, 2) a case in which a robot loses a reference robot from its LOS, 3) a case in which a robot is lost, and 4) a case in which all robots lose the target from their LOS. Results of a simulation and an experiment on prey pursuit show that the proposed self-organization method can be effectively used for multiple mobile robots, despite the use of a simple association rule.

Keywords: Color recognition, LOS, self-organization, singular association.

1. INTRODUCTION

For self-organization of swarm robots, cooperation among swarm robots has been studied by considering wireless communication [1-4]. Cooperation based on ad hoc networks requires localization so that the positions of the robot and its neighboring robots are known. On the other hand, ad hoc networks may be additionally used in vision-based multiple robot systems. In [5], cooperative localization via ad hoc networks in vision-based formation control allows each robot to estimate its relative position and orientation with respect to its neighbors. However, in a self-organization environment where there are many robots and where the robots can adopt many formations, the ad hoc network-based robotic system may need lots of data and a complex communication environment owing to excessive information exchange. The proposed visual cooperation does not require ad hoc networks or localization through the use of an external ceiling camera or beacon systems. It uses the relative distance between robots and their orientation, which are determined with the help of color recognition and a compass sensor, respectively. In this study, self-organization of swarm robots is studied on the basis of a comprehensive treatment of the dynamic association(DA) proposed in [6]. DA algorithms effectively deal with a host of swarming-related issues such as cooperation for fast migration to a target, flexible and agile formation, and inter-agent collision avoidance. In this study, the swarm robot uses the relative position information of a neighboring robot that is in its line of sight, unlike the case of DAs in [6]. This method removes a space constraint and simplifies hardware implementation. The method is similar to path planning for a herd of cows in an open field. In the case where there are no acoustic elements, such animals move with the aid of only sight information, independent of the position information of the entire herd. Two characteristics of their self-organization are as follows: 1) They do not collide with a neighboring cow and obstacles in their line of sight. 2) They migrate to a destination through group behaviors. In this study, these characteristics of the animals are adopted for self-organization. In other words, a swarm robot keeps association not with all neighboring robots, but only with its neighboring robot in the line of sight(LOS), unlike the case of conventional algorithms [6-12]. In the proposed method, the swarm robots are self-organized with the help of neighboring robots with their own vision. In this paper, self-organization means that the swarm robots find a path for group migration while avoiding obstacles, on the basis of LOS visual information. In this study, flexible formation, not static formation [1,7], is employed because of the DA. This paper is an extension of [13], where a framework for decentralized control of swarm systems is presented on the basis of artificial potential functions. In the present study, for swarm robotic systems without a fixed leader robot, experimental self-organization is carried out through visual cooperation. The proposed algorithm uses color information based on vision data. Conventional studies

Manuscript received November 28, 2011; revised June 20, 2012; accepted September 23, 2012. Recommended by Editorial Board member Yangmin Li under the direction of Editor Hyouk Ryeol Choi.

This work was supported by Kyungnam University Foundation Grant, 2010.

Hahmin Jung and Yeongyun Kim are with the Department of Advanced Engineering, Kyungnam University, Changwon, Kyungnam 631-701, Korea (e-mails: zeroful1@naver.com, grantkyg@gmail.com).

Dong Hun Kim is with the Department of Electrical Engineering, Kyungnam University, Changwon, Kyungnam 631-701, Korea (e-mail: dhkim@kyungnam.ac.kr).

* Corresponding author.

have assumed that swarm agents know the position of all neighboring agents, including neighboring agents who are not in the field of view. However the proposed self-organization method involving color recognition considers only the neighboring agents in the LOS by sharing visual information among themselves. Finally, swarm agents reach the final destination by visual assistance among them.

2. ROBOT MODEL AND CONTROL

2.1. Differential-drive robot model

The configuration of a differential-drive robot is completely described by a three-vector, $\mathbf{q}_i = (x_i, y_i, \phi_i)^T$, which defines the current position and orientation in an inertial reference frame. Assuming that the wheel of the robot does not slip on the plane, the motion of the point (x_i, y_i) for robot i is given by [12]

$$\dot{x}_i \sin\phi_i - \dot{y}_i \cos\phi_i = 0 , \tag{1}$$

where (x_i, y_i) is the center of gravity of the robot in the inertially fixed coordinate system and ϕ_i is its orientation. This natural constraint is nonintegrable, i.e., nonholonomic. Hence, the kinematic model is given by

$$\dot{\mathbf{q}}_i = \begin{bmatrix} \dot{x}_i \\ \dot{y}_i \\ \dot{\phi}_i \end{bmatrix} \begin{bmatrix} \cos\phi_i & 0 \\ \sin\phi_i & 0 \\ 0 & 1 \end{bmatrix} \begin{bmatrix} v_i \\ \omega_i \end{bmatrix}. \tag{2}$$

2.2. Trajectory control

A control algorithm for tracking [14] is given by

$$\begin{aligned} v_i &= \gamma \rho_i \cos\Delta\phi_i, \\ \omega_i &= k\Delta\phi_i + \dot{\phi}_{di}, \end{aligned} \tag{3}$$

where $\rho_i = \sqrt{\Delta x_i{}^2 + \Delta y_i{}^2}$, $\Delta x_i = x_{di} - x_i$, $\Delta y_i = y_{di} - y_i$, $\Delta\phi_i = \phi_{di} - \phi_i$, $\phi_{di} = \arctan 2(\Delta y_i, \Delta x_i)$, and $k, \gamma > 0$. $P_{di}(x_{di}, y_{di})$ denotes the desired coordinate trajectories. It can be the path of a virtual leader. As long as P_{di} is bounded, the following inequalities hold:

$$\begin{aligned} &\lim_{t\to\infty} \rho_i(t) \le d, \\ &\lim_{t\to\infty} \| \Delta\phi_i \| \le \delta \end{aligned} \tag{4}$$

for some d, $\delta > 0$ that can be made arbitrarily small with an appropriate choice of the control parameters k and γ. The proof is in [14]. We can formulate the control of a whole system for group migration and obstacle avoidance by using a desired coordinate trajectory.

$$\begin{aligned} x_{di} &= \alpha F_{xi}, \\ y_{di} &= \alpha F_{yi}, \end{aligned} \tag{5}$$

where α is the weight constant of F_{xi} and F_{yi}. $F_i(F_{xi}, F_{yi})$ by potential function is force function, and it is designed by an algorithm that is presented in the next section.

For obtaining neighboring robot position information, the proposed method uses individual vision information instead of communication systems for facilitating communication between robots. This shows that our robot model performs autonomously in a swarm, like bisons in the wild that migrate to a pasture land in a group by using only visual information.

3. APF DESIGN BASED ON COLOR RECOGNITION

The potential function has been designed for group migration, obstacle avoidance, and group formation by the authors of [13], in which a robot was affected by a repulsive field from each obstacle and attractive fields from fellow robots. However, in this study, a robot is affected only by obstacles and a neighboring robot in its LOS and that too within a sensor range. Thus, the configuration of the potential function is very simple, which makes H/W implementation easy. Fig. 1 shows several examples of LOS with a robot, an obstacle, and a target. In Figs. 1(a) and (b), the connection line between the robot R_1 and the obstacle indicates that R_1 can recognize the obstacle. However, the **X** mark implies that the robot does not see the robot R_2 and target. In other words, R_1 does not see the neighboring robot R_2 and the target since the obstacle blocks them in Figs. 1(a) and (b), respectively. Similarly, in Figs. 1(c) and (d), R_1 does not see R_2 and the target since the neighboring robot R_3 blocks them, respectively.

3.1. LOS range of a robot

The LOS range of a robot R_k can be specified by the following set $\mathbf{S}_k = \{R_k \mid \sqrt{(D_x^i - D_x^k)^2 + (D_y^i - D_y^k)^2} \le r, i \ne k\}$, where D_x^k and D_y^k are the x and y coordinates of R_k in a two-dimensional space. D_x^i and D_y^i are the coordinates of a target R_T, neighboring robot R_i, or static obstacle. r is the range of recognition. $\mathbf{I}_k = \{R_k \mid R_k \in \mathbf{S}_k, \overline{R_i R_k}$ *intersects nearby obstacles or neighboring robots*$\}$: $\mathbf{I}_k$ is defined to be such that R_k does not see neighboring robots and a target because of the presence of obstacles, as shown in Fig. 1. $\mathbf{N}_k = \mathbf{S}_k \setminus \mathbf{I}_k$: $\mathbf{N}_k$ is defined to be such that R_k recognizes neighboring robots or a target. The order of the highest robot starts from the 1st robot group. $\mathbf{H}_k = \{R_k \mid R_k \in \mathbf{N}_k,$ *the highest color - ranked robot for* $R_k\}$: $\mathbf{H}_k$ is the highest color-ranked robot in $\mathbf{N}_k$. $\mathbf{T} = \{R_k \mid R_k \in \mathbf{H}_k, \min(\overline{R_i R_k}), R_i$ *is a reference robot or a target*$\}$: $\mathbf{T}_k$ is a target or the reference robot that should follow. For a reference robot, $min(\overline{R_i R_k})$ indicates that R_k follows the nearest robot among the highest ranked robot group. The reference robot is considered as a priority robot that R_k should follow since R_k does not see the target. In particular, R_k is referred to as R_T when it becomes a priority robot. The concept of dynamic association is that R_k follows a single robot having high priority. Thus, Fig. 1(a) shows $R_2 \in \mathbf{I}_1$; Fig. 1(b), $R_T \in \mathbf{I}_1$; Fig. 1(c), $R_2 \in \mathbf{I}_1$ and $R_3 \in \mathbf{T}_1$; and Fig. 1(d), $R_T \in \mathbf{I}_1$ and $R_3 \in \mathbf{T}_1$. The significations of different colors are listed in Table 1.

Table 1. Definition of robot colors.

LED color string	Meaning
1st robot group (red)	Robots seeing the target
2nd robot group (orange)	Robots not seeing the target, but seeing the 1st robot group
3rd robot group (yellow)	Robots not seeing the target and 1st robot group, but seeing the 2nd robot group
4th robot group (green)	Robots not seeing the target and the 1st and 2nd robot groups, but seeing the 3rd robot group
5th robot group (blue)	Robots not seeing the target and the 1st, 2nd, and 3rd robot groups, but seeing the 4th robot group

3.2. APF design

Relative position vectors between the robots and target are defined as

$$\psi_i^k = R_i - T_k, \tag{6}$$

where i is the robot index. Thus, R_i is the robot label and the robot's position is specified by its x and y coordinates. As an example, the vector ψ_1^3 in the context of Figs. 1(c) and (d) is $\psi_1^3 = R_1 - R_3$. ψ_i^T is defined as $\psi_i^T = R_i - R_T$. Attraction toward the target is modeled by attractive fields, which draw a charged robot toward the target in the absence of obstacles. The simple APF for migration is modeled as follows.

$$U_i^a = c_a(1 - e^{-\frac{\|\psi_i^k\|^2}{l_a{}^2}}), \tag{7}$$

where c_a and l_a are the strength and correlation distance for migration. When $\psi_i^k = 0$, U_i^a becomes zero.

Static and moving obstacles are considered. Relative vectors between the robot and obstacles are defined as

$$\psi_i^b = R_i - O_b, \tag{8}$$

where $O_b \in \mathbf{S}_k \setminus \mathbf{T}_k$, b denotes the set of labels for those obstacles that are the objects nearest to robot R_i in the robot's LOS. Collisions between an obstacle and a robot are avoided because of the repulsive force between them. We employ an algorithm that prevents collisions with obstacles by calculating the repulsive potential. A simple APF for obstacle avoidance is modeled as

$$U_i^r = \sum_{b=1}^{n_b} \{c_r e^{-\frac{\|\psi_i^b\|^2}{l_r{}^2}}\}, \tag{9}$$

where c_r and l_r are the strength and correlation distance for obstacle avoidance and n_b is the number of obstacles. The total potential has an additive structure,

$$\begin{aligned} U_i &= U_i^a + U_i^r \\ &= c_a(1 - e^{-\frac{\|\psi_i^k\|^2}{l_a{}^2}}) + \sum_{b=1}^{n_b} \{c_r e^{-\frac{\|\psi_i^b\|^2}{l_r{}^2}}\}. \end{aligned} \tag{10}$$

Its corresponding force is then given by the negative gradient of (10),

$$\begin{aligned} F_i &= -\nabla U_i \\ &= -\frac{2c_a\psi_i^k}{l_a{}^2} e^{-\frac{\|\psi_i^k\|^2}{l_a{}^2}} + \sum_{b=1}^{n_b} \{\frac{2c_r\psi_i^b}{l_r{}^2} e^{-\frac{\|\psi_i^b\|^2}{l_r{}^2}}\}. \end{aligned} \tag{11}$$

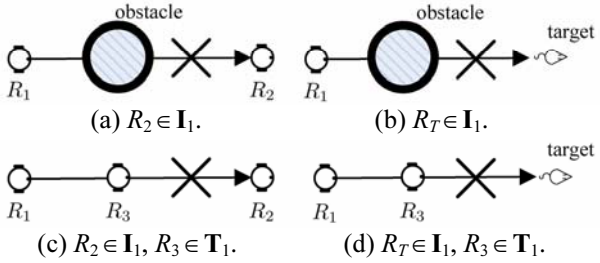

Fig. 1. Example of LOS.

In Section 4, the design and analysis of self-organization based on a color recognition sensor and by using the APF is discussed. x_{di} and y_{di} in (5) are replaced by $F_i(F_{xi}, F_{yi})$ by using the APFs in (11). Then, ρ_i and $\Delta\phi_i$ in (3) are modified and control inputs v_i and ω_i are designed. These control inputs are used in the kinematic model in (2), which describes the motion of the differential-drive robot. For hardware implementation, v_i in (3) is the average of two input voltages to two motors. ω_i is the difference between the two input voltages, i.e., the right and left motor voltages are $V_R = k_v(v_i + \frac{R\omega_i}{2})$ and $V_L = k_v(v_i - \frac{R\omega_i}{2})$, respectively, where R is the diameter of the differential-drive robot and k_v is a voltage proportion constant.

4. SELF-ORGANIZATION BASED ON COLOR RECOGNITION

4.1. Parameter design of APFs

We consider a situation in which two robots are overwhelmed by the potential of a target. Four cases arise when two robots follow the target R_T, as shown in Fig. 2. When the target R_T is in the LOS of R_1 and R_2 and is recognized by them, the two robots are drawn to R_T by an attractive force exerted by R_T. When the two robots try to reach R_T, there is a possibility of a collision occurring between the two robots. Depending on which robot approaches the target earlier and the relative angle between the two robots, there are four possible scenarios (shown in Fig. 2). Two robots approach the target with a small relative angle in Fig. 2(a), with at a relative angle of 90° in Fig. 2(b), and at a relative angle of 180° in Fig. 2(c). Fig. 2(d) shows the case where a robot reaches the target earlier. In order to avoid a collision between the two robots, the attractive field from the target should be eliminated when the distance between R_1 and R_2 is less than d_m, where d_m is the minimum distance that should be maintained between the two robots to avoid a collision. In other words, at robot separation distances less than d_m, the repulsive force of R_1 and R_2 should be larger than the attractive force of the target R_T, i.e., $F_1^r > F_1^a$. Thus,

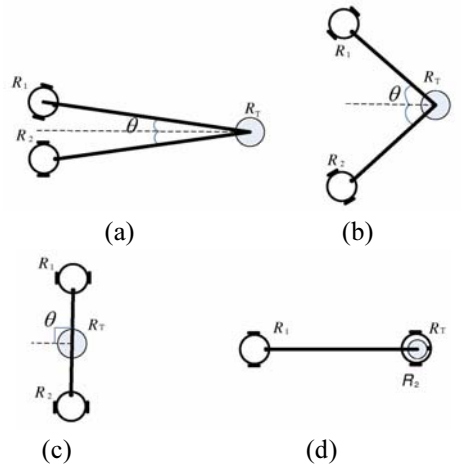

Fig. 2. Cases in which two robots approach the target.

we obtain

$$\frac{2c_r\psi_1^2}{l_r^2}e^{-\frac{\|\psi_1^2\|^2}{l_r^2}} > \frac{2c_a\psi_1^{R_T}}{l_a^2}e^{-\frac{\|\psi_1^{R_T}\|^2}{l_a^2}}. \quad (12)$$

$\psi_1^2 = \frac{d_m}{10}$ and $\psi_1^T = 6d_m$ in Fig. 2(a), $\psi_1^2 = d_m$ and $\psi_1^T = \frac{\sqrt{2}}{2}d_m$ in Fig. 2(b), $\psi_1^2 = d_m$ and $\psi_1^T = \frac{d_m}{2}$ in Fig. 2(c), and $\psi_1^2 = d_m$ and $\psi_1^{R_T} = d_m$ in Fig. 2(d). In order to ensure that the target exerts a strong attractive force, $l_r < l_a$ is chosen. Among the four cases in Fig. 2, rate $\frac{c_r}{c_a}$ has the largest value in the case of Fig. 2(d). Thus, all four cases are satisfied by the following inequality:

$$\frac{c_r}{c_a} > \frac{l_r^2}{l_a^2}e^{\frac{d_m^2}{l_r^2}-\frac{d_m^2}{l_a^2}}. \quad (13)$$

When R_T is not a target but a reference robot, the inequality condition in (15) is reduced since the repulsive force of the reference robot is added. Thus, the inequality condition in (16) is satisfied.

4.2. Self-organized robot using color information

In the swarm platform, the first robot group follows the target, the second robot group follows the first robot group, and so on. The rank composition of the robot group is changed in every time step, depending on whether the LOS has obstacles or neighboring robots. Finally, every sight of robots is shared cooperatively. The robot that does not see the target can also go toward the target and reach it. In this paper, we suppose that an LED color string indicates view status of a robot and a color-detecting sensor is attached to every robot body in the H/W implementation. Table 1 shows the view status of robots for different LED color strings. The more the number of robot groups, the more is the number of different LED color strings required. Next, five cases that may occur in the proposed self-organization are considered.

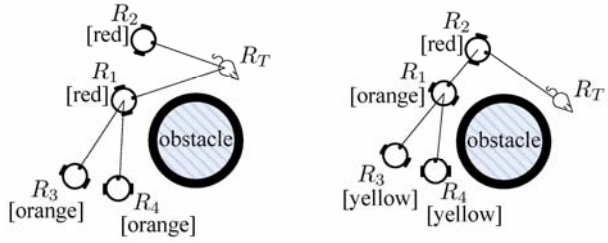

(a) Step [n-1]. (b) Step [n].

Fig. 3. Example of R_1 ($R_T \in \mathbf{I}_1$ after $R_T \in \mathbf{T}_1$).

Case 1. A robot loses the target from its line of sight (Ex. $R_T \in \mathbf{I}_1$ after $R_T \in \mathbf{T}_1$ in Fig. 3)**:** Fig. 3 shows a case in which four robots follow the target. When $R_T \in \mathbf{T}_1$, R_1 is assigned to the first robot group, and its color becomes red. In the next step, when $R_T \in \mathbf{I}_1$, R_1 is assigned to the second group, and its color is changed to orange. R_3 and R_4 are shifted to the third group (orange) from the second group (yellow) since they see a robot from the second group. Finally, even if R_1 does not see the target, it proceeds toward the target by following R_2, which is assigned to the first robot group.

Case 2. A robot loses a reference robot from its line of sight (Ex. $R_1 \in \mathbf{I}_3$ after $R_1 \in \mathbf{T}_3$ in Fig. 4)**:** Fig. 4 shows a case in which five robots move toward the target. When $R_1 \in \mathbf{T}_3$, R_3 is assigned to the second robot group, and its color becomes orange. In the next step, when $R_1 \in \mathbf{I}_3$ and $R_2 \in \mathbf{T}_3$, R_3 is assigned to the third group and its color is changed to yellow. R_4 and R_5 are shifted to the fourth group (green) from the third group (yellow) since they see a robot from the third group. Finally, even if R_3 does not see the target, it moves toward the target by following R_2, which is assigned to the second robot group.

Case 3. A robot is lost (Ex. R_k and $R_T \in \mathbf{I}_5$ after $R_4 \in \mathbf{T}_5$ in Fig. 5)**:** Case 3 is an extension of Case 2. In Fig. 5(a), when $R_4 \in \mathbf{T}_5$, R_5 is assigned to the third robot group and it is yellow. In the next step, $R_4 \notin \mathbf{T}_5$ and $R_k \in \mathbf{I}_5$. In the proposed self-organization, in order that R_5 is not lost, R_5 moves to the position where it last saw R_4. If R_5 does not see any neighboring robots or the target in step $n + 1$ while moving to the last position **A**, it may be lost. Such a case is more likely to occur when either the number of swarm robots is small or obstacles are large. However, the possibility of a robot being lost is not very high. This is because while the lost robot moves to the last position, the possibility of $R_k \in \mathbf{N}_5$ is higher than the possibility of $R_k \in \mathbf{I}_5$. Since the association among swarm

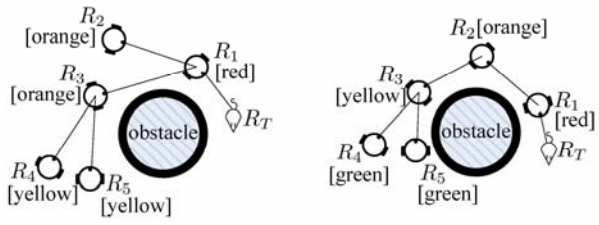

(a) Step [n-1]. (b) Step [n].

Fig. 4. Example of R_3 ($R_1 \in \mathbf{I}_3$ after $R_1 \in \mathbf{T}_3$).

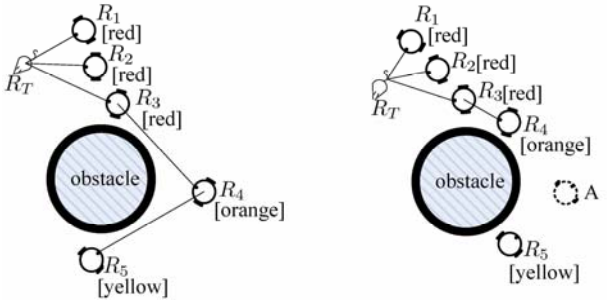

(a) Step [n-1]. (b) Step [n].

Fig. 5. Example of R_5 (R_k and $R_T \in \mathbf{I}_5$ after $R_4 \in \mathbf{T}_5$).

robots can be represented by an incidence matrix [15], case 3 is analyzed by using an incidence matrix in which the association between two robots is set to a node represented by a line. Fig. 5 shows the association of five robots and a target represented by five lines. (14) and (15) show the incidence matrix for Figs. 5(a) and (b), respectively. The column and row vectors consist of $[R_1, R_2, ..., R_T]$ and its associated line. The number of column and row vectors in the incidence matrix is $N \times (N+1)$, where N is the number of swarm robots. In the case of Fig. 5, J consists of 5 × 6 elements since N = 5. In the incidence matrix, the element -1 indicates that the corresponding robot moves toward its neighboring robot or the target R_T, i.e., the robot with -1 is a follower and the robot with 1 becomes a $\mathbf{T}_k$. JJ^T becomes a nonsingular matrix. Thus, the eigenvalues of JJ^T do not contain any zero value. However, in the case of a lost robot, the eigenvalues of $J_{lost}J_{lost}^T$ have at least one zero value since $J_{lost}J_{lost}^T$ becomes a singular matrix.

$$J = \begin{bmatrix} -1 & 0 & 0 & 0 & 0 & 1 \\ 0 & -1 & 0 & 0 & 0 & 1 \\ 0 & 0 & -1 & 0 & 0 & 1 \\ 0 & 0 & 1 & -1 & 0 & 0 \\ 0 & 0 & 0 & 1 & -1 & 0 \end{bmatrix} at\ step\,[n-1]. \quad (14)$$

$$J_{lost} = \begin{bmatrix} -1 & 0 & 0 & 0 & 0 & 1 \\ 0 & -1 & 0 & 0 & 0 & 1 \\ 0 & 0 & -1 & 0 & 0 & 1 \\ 0 & 0 & 1 & -1 & 0 & 0 \\ 0 & 0 & 0 & 0 & 0 & 0 \end{bmatrix} at\ step\,[n]. \quad (15)$$

Case 4. All the robots do not see the target (Ex. $R_T \in \mathbf{I}_2$ after $R_T \in \mathbf{T}_2$ in Fig. 6)**:** Fig. 6 shows that the target is lost from the sight of all robots, similarly to case 3. When $R_T \in \mathbf{T}_2$ in Fig. 6(a), R_2 is assigned to the first robot group and its color becomes red. In the next step, when $R_T \in \mathbf{I}_2$, R_T is out of sight of R_2. Therefore, R_2 goes toward point **A**, where the target was last seen. If the other robots find R_T while R_2 moves to point **A**, then normal self-organization proceeds. The incidence matrix of the example in Fig. 6 is shown in (16) and (17). It is composed similarly to the case of Fig. 5.

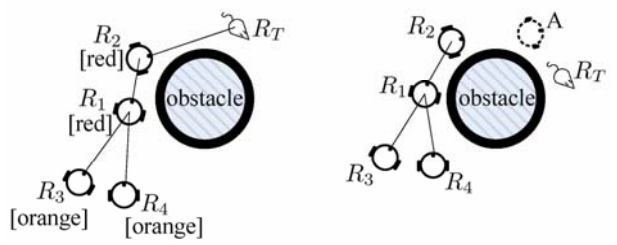

(a) Step [n-1]. (b) Step [n].

Fig. 6. Example of R_2 ($R_T \in \mathbf{I}_2$ after $R_T \in \mathbf{T}_2$).

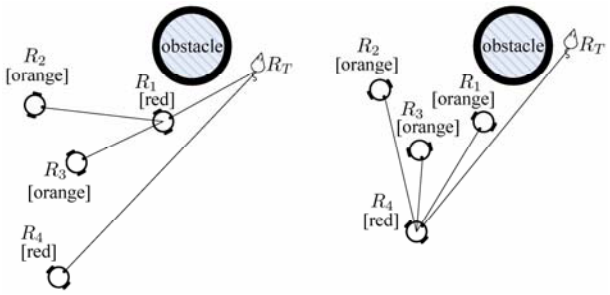

(a) Step [n-1]. (b) Step [n].

Fig. 7. Example of R_1 (going backward from R_T).

$$J = \begin{bmatrix} -1 & 1 & 0 & 0 & 0 \\ 0 & -1 & 0 & 0 & 1 \\ 1 & 0 & -1 & 0 & 0 \\ 1 & 0 & 0 & -1 & 0 \end{bmatrix} at\ step\,[n-1]. \quad (16)$$

$$J_{lost} = \begin{bmatrix} -1 & 1 & 0 & 0 & 0 \\ 0 & 0 & 0 & 0 & 0 \\ 1 & 0 & -1 & 0 & 0 \\ 1 & 0 & 0 & -1 & 0 \end{bmatrix} at\ step\,[n]. \quad (17)$$

Case 5. Robots go toward the higher color-ranked robot that is located behind the target R_T (Ex. $R_4 \in \mathbf{T}_1$ after $R_T \in \mathbf{T}_1$ in Fig. 7)**:** Fig. 7 shows that R_1, R_2, and R_3 go behind R_T. In Fig. 7(a), R_1 and R_4 are assigned to the first group. In the next step, $R_T \in \mathbf{I}_1$ and $R_4 \in \mathbf{T}_1$. The other robots are $R_4 \in \mathbf{T}_2$ and $R_4 \in \mathbf{T}_3$, as shown in Fig. 7(b). In this situation, robots other than R_4 go away from R_T since they follow R_4 located far from R_T. If R_4 does not see R_T after R_T moves behind the obstacle, the situation is the same as that in Case 4. Subsequently, R_1 goes forward to the previous position where the target was seen, since $R_T \notin \mathbf{N}_1$ and $\psi_i^T < \psi_4^T$ in the preset step and since the self-organization scheme is designed such that a lower color-ranked robot follows the highest color-ranked robot according to the color-rank rule in Table 1.

5. SIMULATION

The cooperative nature of the foraging activity is motivated by biological requirements. Each robot in this task aims to reach a moving target, while avoiding obstacles, keeping away from colliding with neighboring robots, and finally swarming to the target. Figs. 9(a) and

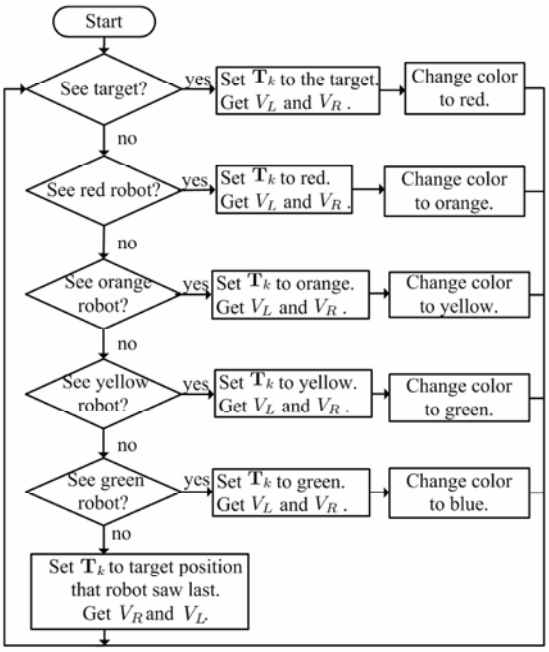

Fig. 8. Procedure for the proposed self-organization.

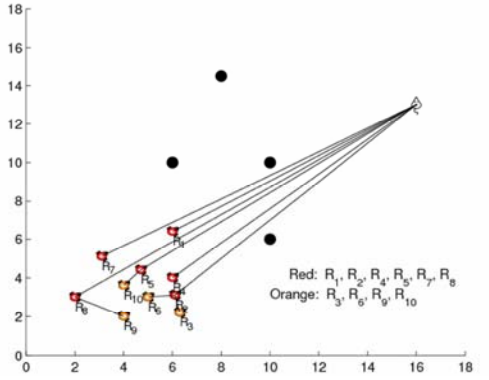

(a) Step 1.

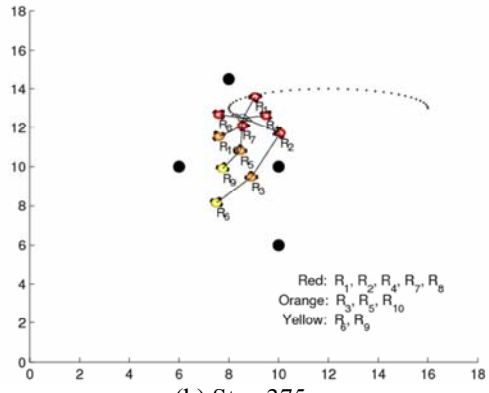

(b) Step 375.

Fig. 9. Snapshots of singular association.

(b) show snapshots of simulation results at several steps. In the simulations, the LOS of each robot is considered and all the robots do not know the target position until the target is in the LOS. In Fig. 9, lines between robots indicate association for self-organization; the moving target is a mouse, and the four close circles are obstacles. In Fig. 9(a), 10 robots are initialized on the bottom-left side of the simulation environment. The robots seeing the target are then assigned to the first robot group (red), and they go toward the moving target. The other robots not seeing the target are assigned to the second robot group (orange), and they follow their reference robot. In Fig. 9(b), R_9, which is assigned to the third robot group (yellow), goes toward the target even if it does not see the target. Finally, all the robots reach the target with the help of visual cooperation of neighboring robots, while maintaining a minimum distance with neighboring robots to avoid collisions. Fig. 10 shows the forces, given by (14), exerted on five selected robots. The movie file of the simulation is shown on You Tube [16].

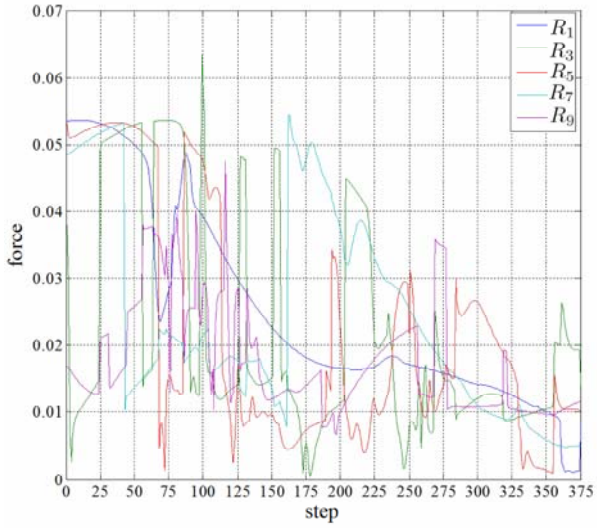

Fig. 10. Forces exerted on five selected robots.

6. EXPERIMENT

This section presents an experiment results on skid-steering mobile robots (SSMRs) performed with the purpose of verifying the effectiveness of the proposed visual cooperation based on color recognition. The conventional swarm systems use a ceiling camera or more than three beacons for determining robot positions, where the beacon involves radio frequency transfer. However, in this paper, an experiment on a prey pursuit mission involving color recognition by a color tracking sensor (CTS) is performed. In the experiment, the CTS tracks colors by using only a luminous source. Thus, general colors such as those of peripheral things are not considered in the vision of the robot. The purpose of this study, in which a simple control strategy, color recognition, LOS, and a singular association rule are used, is to propose a practical approach suitable for H/W implementation while overcoming constraints faced in actual H/W implementation.

6.1. Experimental setup

The SSMR used in the experiment has four DC motors and a system board. All robots have the same size (33.8 cm × 32.5 cm × 61 cm) in Fig. 11. The upper part of a robot includes an omnidirectional mirror, a color

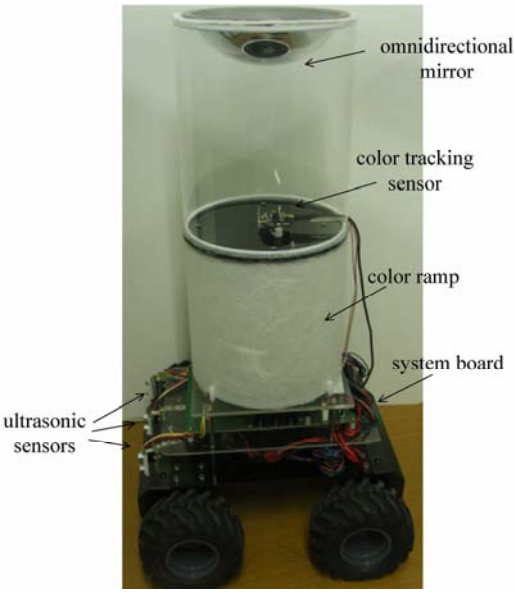

Fig. 11. The proposed SSMR.

tracking sensor, and a color lamp with full color LEDs. The target R_T is controlled through Bluetooth communication by a user. All SSMRs are autonomously moved by the proposed method.

6.2. Control method of SSMR

Five homogeneous SSMRs (Fig. 12) are used in the experiment, instead of differential-drive robots. In Fig. 12, P_{LF}, P_{RF}, P_{LR}, and P_{RR} stand for pulse width modulation (PWM) duty cycles on the front-left, right, rear-left, and right wheels, respectively. The average signals of the left and right wheels are $P_L = \frac{P_{LF}+P_{LR}}{2}$ and $P_R = \frac{P_{RF}+P_{RR}}{2}$, respectively. For the forward movement of the robot, the average signal requires $P_L > 0$, $P_R > 0$, and $P_L = P_R$. For $P_L < 0$, $P_R < 0$, and $P_L = P_R$, the robot moves backward. The difference between P_L and P_R makes the robot rotate. For $P_L > 0$ and $P_R > 0$, $P_L > P_R$ and $P_L < P_R$ make the robot rotate right and left, respectively. If the sign of the two signals is different, the robot makes a standing turn. The obstacles in front of the robot are recognized by three ultrasonic sensors. The recognition range of the ultrasonic sensors is set to be up to 1 M, and the time taken by them to detect obstacles is about 212 ms. The CTS is used for tracking the target position. The time taken by the CTS is 160 ms. The CTS can track color within a distance of ± 2 M from the center of the robot. Each robot finds its own neighboring robot within a short distance, or a real target. Bluetooth communication is used by the user to confirm the robot state and to debug it. Low-cost hardwares appropriate for the swarm robot concept are chosen. The robot is equipped with two AVR microcontroller units (MCUs), with one being used for motor control and the other for computations related to the CTS and Bluetooth communication. The total sampling time for actuating the robot is 360 ms.

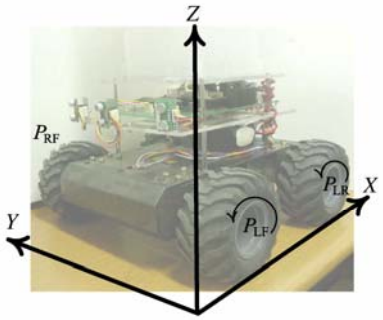

Fig. 12. SSMR.

6.3. Experimental results

In the experiment, the five robots are expected to catch a moving target and simultaneously avoid some moving or stationary obstacles. The moving obstacles are neighboring robots and the stationary obstacles are the two fixed boxes shown in Fig. 13. The experimental result is shown in Fig. 13; eight photos (a)-(h) taken during the experiment are shown, and the design parameters are set to $r = 2$, $c_a = 1$, $l_a = 15$, $c_r = 0.5$, and $l_r = 0.3$. The target R_T moves with a constant velocity

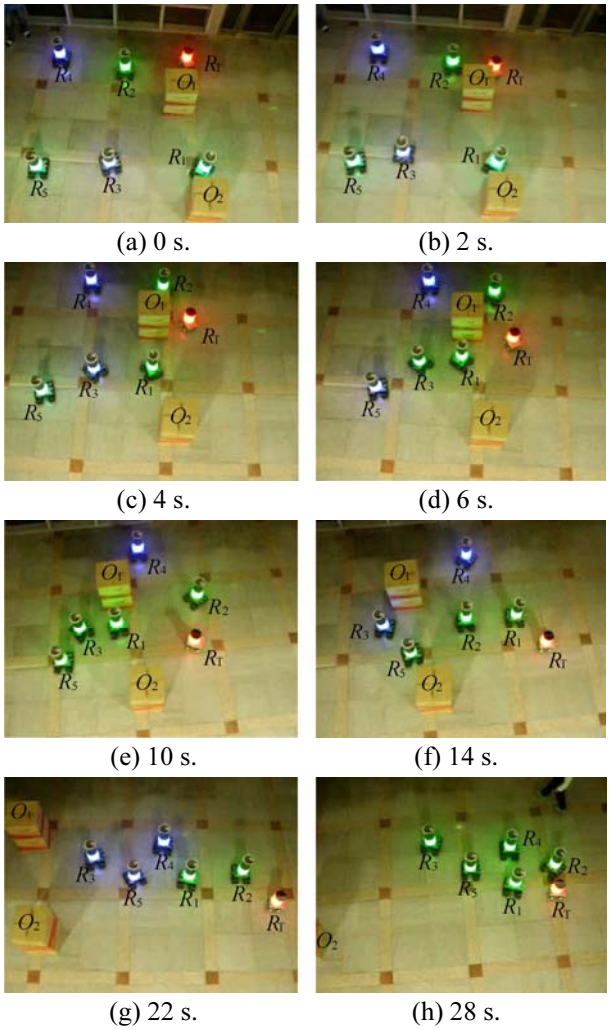

(a) 0 s. (b) 2 s.

(c) 4 s. (d) 6 s.

(e) 10 s. (f) 14 s.

(g) 22 s. (h) 28 s.

Fig. 13. Experimental result of prey pursuit [17].

Table 2. Change in priority of the robot groups in Fig. 13.

Steps	1st robot group	2nd robot group	3rd robot group
(a)	R_2	R_3, R_4	R_1, R_5
(b)	R_2	R_3, R_4	R_1, R_5
(c)	R_1, R_2	R_3, R_4	R_5
(d)	R_1, R_2, R_3	R_4, R_5	*none*
(e)	R_1, R_2, R_3, R_5	R_4	*none*
(f)	R_1, R_2, R_5	R_3, R_4	*none*
(g)	R_1, R_2	R_3, R_4, R_5	*none*
(h)	R_1, R_2, R_3, R_4, R_5	*none*	*none*

less than the maximum velocity of the five robots. Table 2 shows the change in the priority of robot groups at the time steps corresponding to the photos in Fig. 13. The experimental results confirm that the proposed self-organization method based on color recognition can be effectively used for the prey pursuit of multiple mobile robots. A movie file of the experiment can be found in [17].

7. CONCLUSIONS

This is the first attempt where visual cooperation has been considered for self-organization of swarm robots. The paper presents a self-organization scheme for swarm robots, based on color recognition and LOS. The self-organizing scheme for conventional swarm systems requires communication between robots and a central computer since it use a ceiling camera as an example of conventional robot soccer or beacon systems, which need limited indoor space. The main advantages of the proposed scheme are as follows: 1) it does not require indoor space, 2) it does not involve wireless communication between robots and a main PC, and 3) it does not involve information exchange among fully connected neighboring robots. The benefits are a consequence of the use of color recognition in the LOS among robots to realize self-organization. Another key feature is the introduction of singular association that considers exchange of visual information only between a robot and its reference robot or a target, not plural association involving exchange of fully connected visual information among many robots. Extensive simulation and experimental results have been presented to show the viability and effectiveness of the proposed self-organization.

REFERENCES

[1] A. K. Das, R. Fierro, V. Kumar, J. P. Ostrowski, J. Spletzer, and C. J. Taylor, "A vision-based formation control framework," *IEEE Trans. on Robotics and Automation*, vol. 18, no. 5, pp. 813-825, 2002.

[2] J. Desai, V. Kumar, and J. P. Ostrowski, "Control of changes in formation for a team of mobile robots," *Proc. of the IEEE International Conference on Robotics and Automation*, vol. 2, pp. 1556-1561, 1999.

[3] X. Chen and Y. Li, "Smooth formation navigation of multiple mobile robots for avoiding moving obstacles," *International Journal of Control, Automation, and Systems*, vol. 4, no. 4, pp. 466-479, 2006.

[4] S. Carpin and L. E. Parker, "Cooperative leader following in a distributed multi-robot system," *IEEE Trans. on Robotics and Automation*, vol. 3, pp. 2994-3001, 2002.

[5] J. Spletzer, V. Kumar, and C. Taylor, "Ad hoc networks for localization and control," *Proc. of the 41st IEEE Conference on Decision and Control*, vol. 3, pp. 2978-2983, 2002.

[6] G. Ye, H. O. Wang, K. Tanaka, and Z. Guan, "Managing group behaviors in swarm systems by associations," *Proc. of the 25th American Control Conference*, pp. 3537-3544, 2006.

[7] D. Minor and M. Desjardins, "Predicting and controlling system-level parameters of multi-agent systems," *Proc. of AAAI Fall Symposium on Complex Adaptive Systems and the Threshold Effect*, pp. 92-05, 2009.

[8] T. Balch and R. C. Arkin, "Behavior-based formation control for multirobot teams," *IEEE Trans. on Robotics and Automation*, vol. 14, no. 6, pp. 926-939, 1998.

[9] J. Sullivan, S. Waydo, and M. Campbell, "Using stream functions for complex behavior and path generation," *Proc. of the AIAA Guidance, Navigation and Control Conference*, pp. 3-5, 2003.

[10] V. Gazi and K. M. Passino, "Stability analysis of social foraging swarms," *IEEE Trans. on Systems*, vol. 34, no. 1, pp. 539-557, 2004.

[11] S. S. Ge and Y. J. Cui, "Dynamic motion planning for mobile robots using potential field method," *Autonomous Robots*, vol. 13, no. 3, pp. 207-222, 2002.

[12] D. H. Kim and S. H. Han, "Robust self-organization for swarm robots," *Proc. of International Conference on Control, Automation and Systems*, pp. 1228-1233, 2008.

[13] D. H. Kim, H. O. Wang, and S. Shin, "Decentralized control of autonomous swarm systems using artificial potential functions: analytical design guidelines," *International Journal of Intelligent and Robotic Systems*, vol. 45, no. 4, pp. 369-394, 2006.

[14] M. Egerstedt and X. Hu, "Formation constrained multi-agent control," *IEEE Trans. on Robotics and Automation*, vol. 17, no. 6, pp. 947-951, 2001.

[15] G. S. Willium, *Introduction to Linear Algebra*, 4th ed., Wellesley-Cambridge Press, Wellesley, MA, February, 2009.

[16] http://www.youtube.com/watch?v=_cHlB1ShQlM

[17] http://www.youtube.com/watch?v=nBGRRXOQge0

Hahmin Jung received his B.S. and M.S. degrees from the Division of Electrical and Electronic Engineering and the Department of Advanced Engineering, Kyungnam University, Korea, in 2009 and 2011, respectively. He is currently a Ph.D. candidate in the Department of Advanced Engineering from Kyungnam University. His research interests include swarm robots, localization, and behavior algorithms.

Yeongyun Kim received his B.S. and M.S. degrees from the Division of Electrical and Electronic Engineering and the Department of Advanced Engineering, Kyungnam University, Korea, in 2009 and 2012, respectively. He is currently a Ph.D. candidate in the Department of Advanced Engineering from Kyungnam University. His research interests include swarm robots, mobile robots, localization, and behavior algorithms.

Dong Hun Kim received his B.S., M.S., and Ph.D. degrees from the Department of Electrical Engineering, Hanyang University, Korea, in 1995, 1997, and 2001, respectively. From 2001 to 2003, he was a research associate under several grants in the Department of Electrical and Computer Engineering, Duke University, NC, USA. In 2003, he joined Boston University, MA, USA, as a visiting assistant professor under several grants at the Department of Aerospace and Mechanical Engineering. In 2004, he was engaged in post-doctoral research at the School of Information Science and Technology, the University of Tokyo, Japan. Since 2005, he has been an associate professor at the Department of Electrical Engineering, Kyungnam University, Korea. His research interests include swarmintelligence, self-organization of swarm systems, mobile robot path planning, decentralized control of autonomous vehicles, intelligent control, and adaptive nonlinear control.